# INFLUENCE OF ANIMAL SLURRY ON CARBON C35 STEEL WITH DIFFERENT MICROSTRUCTURE AT ROOM TEMPERATURE

**Tomasz Lipinski[1], Jacek Pietraszek[2]**
[1]University of Warmia and Mazury in Olsztyn, Poland; [2]Cracow University of Technology, Poland
tomaszlipinski.tl@gmail.com, jacek.pietraszek@mech.pk.edu.pl

**Abstract.** Steels are the basic construction materials used in machine building, construction and in the construction industry. These materials often work in contact with aggressive factors. When subjected to corrosion, they go to their natural oxidation state. Mainly carbon steel C35 is intended for quenching and tempering. The steel is most often used for the production of tools and machine elements that are subject to medium loads and at the same time are very resistant to abrasion. Different heat treatment conditions result in different microstructural structure of C35 steel, and therefore also its different properties, including corrosive ones. The corrosion of these steels is easy to control. It is usually superficial. One of the more complex corrosive environments is animal slurry. As a result, the corrosive effects of animal slurry are complex and time-varying. Slurry is a mixture of dung and urine. The aggressive corrosive constituents in slurry are urea, uric acid, naturally excreted chloride as well as ammonia or ammonium salts. The purpose of this article is to investigate corrosion resistance in different time (48, 96, 144, 192, 240, 288, 336 and 432 hours) using weight loss and profile roughness parameters of structural steel in grade C45 in natural water solution of animal slurry at room temperature (25ºC). The tests were carried out for steel subjected to normalizing annealing as well as hardening and tempering at 300ºC. In order to be able to compare the corrosion rate of stainless steels with steel C35, it was decided to carry out the tests based on the methodology of testing corrosion-resistant steels. Corrosion tests show that the tested steel in animal slurry as a corrosive environment is characterized by a different corrosion rate, the measure of which for C35 steel may be the surface roughness.

**Keywords:** animal slurry, carbon steel, corrosion, corrosion rate, roughness.

## Introduction

Materials intended for building structures and elements of agricultural machinery should ensure not only aesthetic appearance, but also the safety of people and objects during use [1-9]. C35 steel is one of the most popular non-alloy steels. It is often used in various types of constructions, also periodically working in contact with aggressive media. C35 steel contains from 0.32% to 0.39% C and, in small amounts, of silicon, manganese, chromium, nickel, molybdenum, copper, sulphur and phosphorus. All the chemical elements and different heat treatment conditions it contains affect the mechanical, physical and chemical properties of steel, including corrosion resistance. Due to its low cost and high efficiency, steel grade C35 is widely used in agriculture, construction and engineering for structural components. This steel is mainly used in the form of bars and sections in steel structures, as well as in the production of various machine parts, such as shafts, cylinders, gear wheels, axles, discs, traverses, etc. The development of corrosion-resistant steels resulted in the gradual displacement of carbon steels from application in structures operating in an aggressive environment [10-20]. Nevertheless, economic factors predispose these steels to further use in harsh environments.

Elements of machines and devices used in agriculture and agricultural constructions are in contact with an aggressive corrosive environment during their work included in animal slurry and its aqueous solutions. Animal manure products that occur naturally in the farm atmosphere, such as chloride fumes, NOx and SOy, HzS and others, should also be considered. Slurry is a mixture of dung and urine, and farmyard manure etc. The corrosive constituents in slurry are first of all: ammonia and its salts, urea, uric acid, naturally excreted chloride [21-31].

Artificial fertilizers and animal slurry are the basic corrosive environments faced by structures, machinery and technical facilities used in agriculture. Considering the importance of corrosion resistance of steel to animal slurry as the basic corrosive factor in agriculture, it was decided to test the corrosion rate of C35 low-carbon structural steel in an aqueous solution of animal slurry under normal temperature conditions (room temperature). The issues and conclusions contained in this article may be of interest to both researchers-practitioners in the field of materials science [32-34], related management [35, 36], and researchers involved in the implementation of new methods of data analysis [37; 38]. This paper presents the corrosion tests of normalizing annealing as well as hardening and tempering at 300 ºC and is an extension of the tests presented in [27-28] for the alloy from the same group not cold worked.

## Materials and methods

The research was performed on carbon C35 (1.0501) steel flat bar $t = 8.00$ mm thickness with chemical composition according to the PN-EN ISO 683-1:2018-09 [39]. The actual chemical composition of steel consists of: 0.36% C, 0.22% Si, 0.54% Mn, 0.024% P, 0.26% S, 0.16% Cr, 0.19% Cu, 0.21% Ni and 0.002% N. The specimens from the steel flat bar $t = 8.00$ mm thickness were cut samples by a mechanical saw to size 40 x 10 mm (area of 16 $cm^2$). Next the samples were ground on the grinding wheel successively from $R_a = 0.36$ to $R_a = 0.44$ μm. The samples made of C35 steel, after preparation, were subjected to normalizing annealing at the temperature of 880 ºC and austenitizing time of 8 minutes and cooling in air, and then hardening from the temperature of 860 ºC with cooling in water. Immediately after hardening, the samples were tempered at the temperature of 300°C for 2.5 hours with air cooling. After heat treatment, the samples were ground on sandpaper, obtaining the roughness as before the heat treatment. The samples were rinsed and cleaned by 95% $C_2H_5OH$ before the samples were soaked in the corrosive. The samples despite the tempered martensitic microstructure (Fig. 1) were tested in accordance with the standard dedicated for stainless steel PN-EN ISO 3651-1:2004 [40]. Taking into account the more and more frequent use of corrosion-resistant steels in an aggressive environment, it was decided to apply the criteria describing the corrosion process provided for corrosion-resistant steels. This approach will make it possible to compare the corrosion parameters of carbon steels and corrosion-resistant steels. The corrosive mixture was prepared as an aqueous solution of 80% animal slurry with the composition shown in Table 1 and 20% distilled water. Both components were measured by volume. The corrosion rate of the steel was determined by measuring the weight loss.

Table 1

**Mean chemical compositions of animal slurry and parameters**

| **P, mg·L$^{-1}$** | **K, mg·L$^{-1}$** | **Mg, mg·L$^{-1}$** | **Ca, mg·L$^{-1}$** | **Na, mg·L$^{-1}$** | **Zn, mg·L$^{-1}$** | **$NO_3$, mg·L$^{-1}$** |
|---|---|---|---|---|---|---|
| 175 | 158 | 6.4 | 39.2 | 102 | 0.41 | 35 |

| **PH** | ***EC*, mS·cm$^{-2}$** | ***BOD*, mg·L$^{-1}$** | ***COD*, mg·L$^{-1}$** | ***TKN*, g·L$^{-1}$** |
|---|---|---|---|---|
| 6.7 | 5.86 | 2350 | 2980 | 1.82 |

Note: *EC* – electric conductivity, *BOD* – biochemical oxygen demand, *COD* – chemical oxygen demand, *TKN* – total kjeldahl nitrogen

The corrosion rate of S235JR steel measured in mm per year was calculated with the use of the below formula (1), measured in g·m$^{-2}$ was calculated with the use of the below formula (2):

$$r_{corm} = \frac{8760 \cdot m}{S \cdot t \cdot \rho}, \tag{1}$$

$$r_{corg} = \frac{10000 \cdot m}{S \cdot t}, \tag{2}$$

where $t$ – time of treatment in a corrosive solution of boiling nitric acid, hours;
$S$ – surface area of the sample, $cm^2$;
$m$ – average mass loss in boiling solution, g;
$\rho$ – sample density, g·cm$^{-3}$.

The influence of animal slurry on the C35 carbon steel corrosion resistance was investigated using the weight loss. The mass of samples was measured by the Kern ALT 3104AM general laboratory precision balance with accuracy of measurement 0.0001 g. The time range of the research was: 48, 96, 144, 192, 240, 288, 336, 384 and 432 hours.

Profile roughness parameters were analyzed by the Diavite DH5 profilometer for which the maximum length of the measuring section is $l_t = 15$ mm (evaluation length plus start and finish lengths) (limitation of the measuring instrument). The evaluation length (ln) was dependent on the $R_a$ parameter, for the soaking time 48 and 96 hours $l_n = 4$ mm, for the soaking time from 144 hours $l_n = 12.5$ mm. The tracing speed was 0.25 mm·s$^{-1}$.

## Results and discussion

The microstructure of C35 steel in delivery condition is presented in Fig. 1 (medium-tempered martensite) and the Abbott curve surface profilogram of C35 steel after corrosion tests in animal slurry at room temperature for the time 432 hours is presented in Fig. 2.

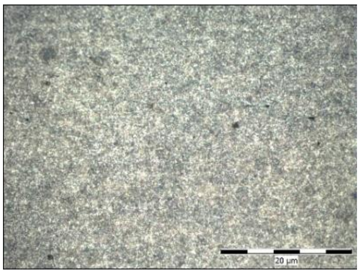

Fig. 1. **Microstructure of C35 steel in delivery condition, etched with Nital**

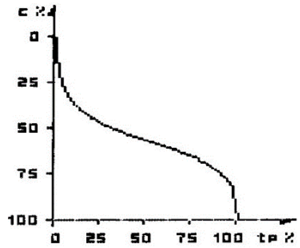


Fig. 2. **Abbott curve surface profilogram of C35 steel after corrosion tests in animal slurry at room temperature for 432 hours (Fig. 3)**

Profile roughness parameters of C35 steel after corrosion tests in animal slurry at room temperature for 432 hours are presented in Fig. 3.

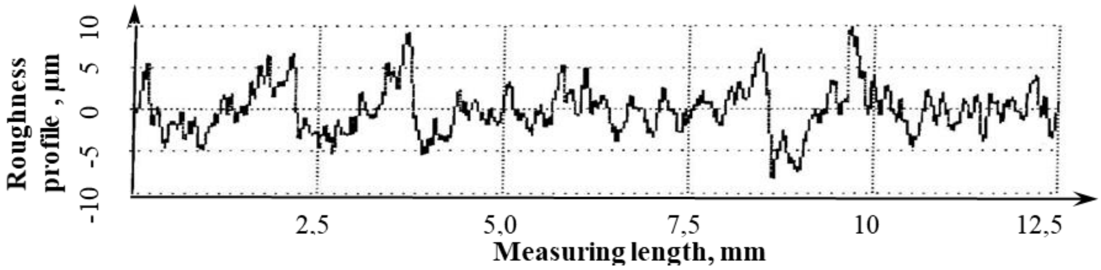


Fig. 3. **Profile roughness of C35 steel after corrosion tests in animal slurry at room temperature for 432 hours**

Profile roughness parameters of C35 carbon steel for different corrosion time with the determination coefficient are presented in Fig. 4 for $R_a$ and $R_q$ and in Fig. 5 for $R_t$ and $R_p$. Changes to all profiles of roughness of C35 quenching and tempered at the temperature of 300 ºC after corrosion tests in animal slurry at room temperature for different corrosion time can be represented with sufficient accuracy by a polynomial function (Fig. 4-5).

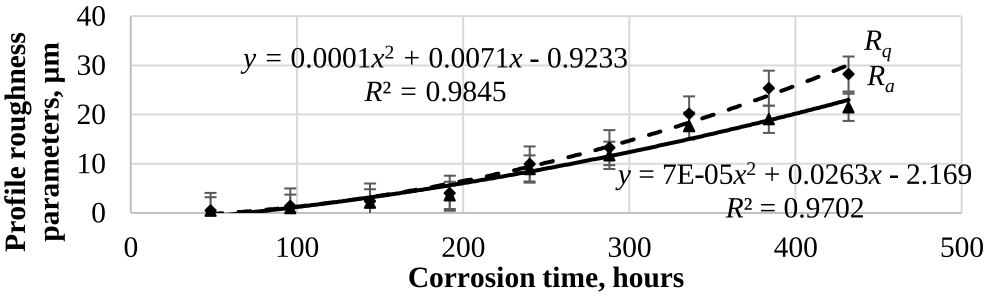


Fig. 4. **Profile roughness of C35 steel after corrosion tests in animal slurry at room temperature for different corrosion time:** *R*a – arithmetical mean roughness value, µm; $R_q$ – mean peak width, µm

The corrosion rate and roughness profile of the steel consists of three periods Fig. 4-Fig. 5. The first, in which the increase in the corrosion rate and surface roughness is low. The second, where there is a faster increase in roughness and corrosion speed. The third, in which the roughness and corrosion speed are stabilized [24; 30-31]. To emphasize all three corrosion periods, the results are presented in the form of fourth order polynomials. In order to relate the corrosion results to the proportional function, line graphs were also plotted.

Percentage effects of the corrosion time on the relative mass loss (RML) of C35 carbon steel after corrosion tests in animal slurry at room temperature (Fig. 6) is sufficiently accurately described by a second degree polynomial function. In progress of keeping the steel in the aqueous solution of animal slurry, a slow increase in the mass corrosion loss was noted. Over time, the weight loss was faster and faster. This relationship is confirmed by the change of the Ra parameter (Fig. 4). Up to approximately 144 hours of soaking the steel, the increase in the corrosion rate was linear. With increasing the soaking time, greater dynamics of the increase in the weight loss with the passage of time was observed.

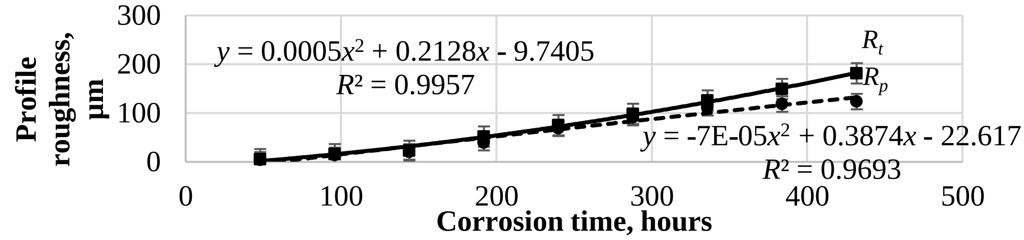


Fig. 5. **Profile roughness of C35 steel after corrosion tests in animal slurry at room temperature for different corrosion time:** $R_p$ – maximum roughness depth, µm; $R_t$ – total height of the roughness profile, µm

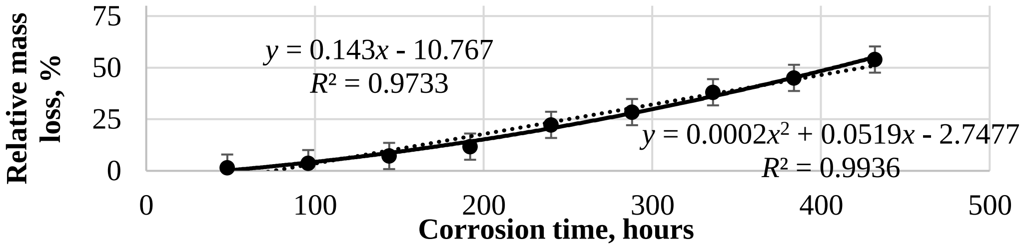


Fig. 6. **Percentage effects of the corrosion time on the relative mass loss (RML) of C35 carbon steel after corrosion tests in animal slurry at room temperature**

The effect of corrosion time on the corrosion rate measured in mm per year of C35 steel after corrosion tests in animal slurry at room temperature with determination coefficient is presented in Fig. 7 and in gram per $m^2$ in Fig. 8.

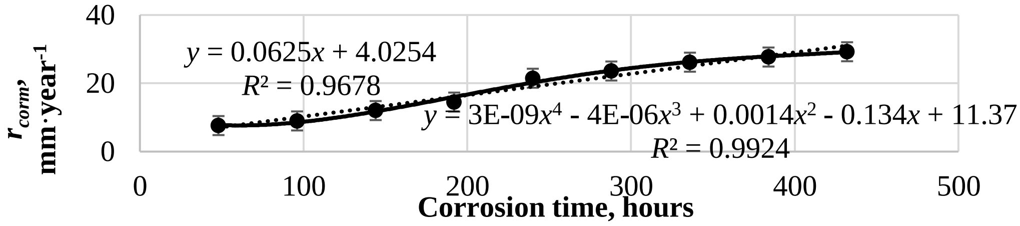


Fig. 7. **Effect of the corrosion time on the corrosion rate measured in mm per year of C35 steel after corrosion tests in animal slurry at room temperature**

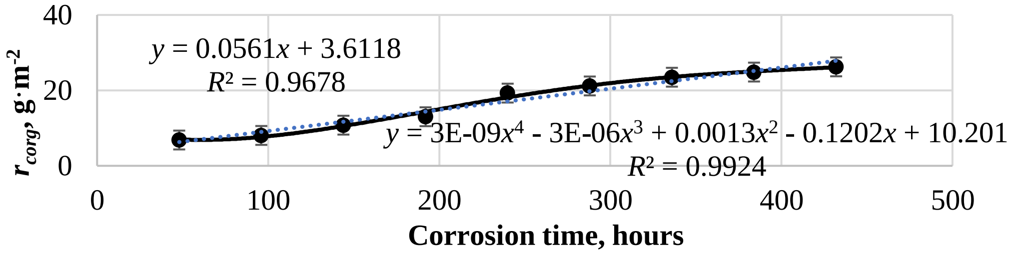


Fig. 8. **The effect of the corrosion time on the corrosion rate measured in gram per $m^2$ of C35 steel after corrosion tests in animal slurry at room temperature**

On the basis of the analysis of changes in the surface roughness parameters (Fig. 4 and Fig. 5) and the corrosion rate (Fig. 7 and 8), smooth transitions between the individual stages of corrosion were found. A similar curve of the course of corrosion was described in [24]. However, the authors did not distinguish the third period of corrosion, although it occurs in 4 out of 5 presented curves. Nevertheless, three periods of corrosion can be distinguished. The first period ends after 144 hours of soaking the steel and the second period after 288 hours. Based on the results of the research presented in this paper and the results of the research presented in [39-40], it was found that animal slurry at room temperature is an aggressive corrosive medium for steel from the C35 group. The slower corrosion rate was achieved for shorter soaking times and therefore for penetrating the steel surface layer. This is most likely due to the greater hardness of the steel after hardening and tempering.

## Conclusions

1. Animal slurry with a room temperature is an aggressive corrosive medium for the steel grade C35.
2. A gentle transition between the various stages of corrosion was noted, which is reflected in the surface roughness and corrosion velocity. In the first stage of soaking the samples (up to 144 hours), the corrosion rate is slow and linear. After lengthening the soaking time, the course of the corrosion process is well reflected by the second degree curve. It proves the increase in the corrosion rate of C35 steel.
3. After soaking the steel for 432 hours, an increase in the roughness parameters (approx.) $R_a$ from 0.4 to 21 μm, $R_q$ from 0.5 to 28 μm, $R_p$ from 4.2 to 123 μm and $R_t$ from 5.5 to 181 μm and an increase in the corrosion rate from 7 to 29 $mm \cdot year^{-1}$ and 6 to 26 $g \cdot m^{-2}$ are observed.
4. Determining the corrosion rate using the methodology used for corrosion-resistant steel can assist designers in rationally selecting the material of constructions.

## Author contributions

Conceptualization, T.L.; methodology, T.L.; validation, J.P. and T.L.; formal analysis T.L.; writing and editing, J.P. and T.L.; All authors have read and agreed to the published version of the manuscript.

## References

[1] Ulewicz R., Mazur M., Bokůvka O. Structure and mechanical properties of fine-grained steels. Periodica Polytechnica Transportation Engineering 41(2), 2013 pp. 111-115.
[2] Blikharskyy Z., Bruzda K., Selejdak J. Effectivenes of Strengthening Loaded RC Beams with FRCM System. Archives of Civil Engineering 64(3), 2018, 3 – 13.
[3] Vicen M., Bronček J., Nový F. Investigation of tribological properties of CarbonX coating deposited on 100Cr6 steel, Production Engineering Archives, 25(25), 2019, pp. 52-55.
[4] Bricín D., Kříž A. Influence of the Boriding Process on the Properties and the Structure of the Steel S265 and the Steel X6CrNiTi18-10. Manufacturing Technology 21(1), 2021, pp. 37-44.
[5] Nová I., Machuta J. Monitoring of the diffusion processes during carburizing automotive steel parts. Manufacturing Technology, 16(1), 2016, pp. 225-230.
[6] Korzekwa, J., Skoneczny, W., Dercz, G., Bara, M. Wear mechanism of Al2O3/WS2 with PEEK/BG plastic. Journal of Tribology, 136(1), 2014, art. 011601.
[7] Hren I., Kusmierczak S., Kurajdová K., Luňák M. Analysis of the influence of surface condition on the corrosion behavior of alloy 2024. Manufacturing Technology 20(5), 2020, pp.603-611.
[8] Lipiński T. Investigation of corrosion rate of X55CrMo14 stainless steel at 65% nitrate acid at 348 K. Production Engineering Archives Volume 27, Issue 2, September 2021, pp. 108-111.
[9] Selejdak J., Blikharskyy Y., Khmil R., Blikharskyy Z. Calculation of Reinforced Concrete Columns Strengthened by CFRP. In: Blikharskyy, Z., Koszelnik, P., Mesaros, P. (eds) Proceedings of CEE 2019. CEE 2019. Lecture Notes in Civil Engineering vol 47. 2020, pp. 400-410.
[10] Lipiński T. Corrosion effect of 20% NaCl solution on basic carbon structural S235JR steel. 15th International Scientific Conference Engineering for Rural Development, Jelgava, 24-26.05.2017. Proceedings, vol. 15, pp. 1069-1074.
[11] Selejdak J., Khmil R., Blikharskyy Z. The influence of simultaneous action of the aggressive environment and loading on strength of RC beams. 12th International Conference Quality Production Improvement, Zaborze, Poland 18-20 June 2018, MATEC Web of Conferences Vol. 183, 02002/2018, 6s.

[12] De Belie N., at all Durability of building materials and components in the agricultural environment, Part II: metal structures. J. Agric. Eng. Res., 75, 2000, pp. 333-347.
[13] Szabracki P., Lipiński T. Effect of aging on the microstructure and the intergranular corrosion resistance of X2CrNiMoN25-7-4 duplex stainless steel. Solid State Phenomena, 203-204, 2013, pp. 59-62.
[14] Zatkalíková V., Markovičová L. Influence of temperature on corrosion resistance of austenitic stainless steel in Cl− containing solutions. Production Engineering Archives, 25, 2019, pp. 43-46.
[15] Uhlig H.H., Revie R.W. Corrosion and corrosion control. 3rd Edition, John Wiley and Sons 1985.
[16] Lipiński T. Corrosion resistance of 1.4362 steel in boiling 65% nitric acid. Manufacturing Technology, 16 (5), 2016, pp. 1004-1009.
[17] Kusmič D., Faltejsek P. Corrosion resistance of low temperature plasma nitrided X12CrMoWVNbN10-l-l martensitic stainless steel. Manufacturing Technology, 19(4), 2019, pp. 619-623.
[18] Lipiński T. Corrosion rate of the X2CrNiMoN22-5-3 duplex stainless steel annealed at 500 degrees C. Acta Physica Polonica A,130 (4), 2016, pp. 993-995.
[19] Duryahina Z.A., Makhorkin I.M., Lazko H.V., Bychynskyi V.I. Evaluation of temperature fields in corrosion-resistant steels under the action of laser radiation. Materials Science, 43(6), 2007, pp. 800-806.
[20] Blatnická M., Blatnický M., Dižo J, Sága M. Comparison of analytical stress analysis and numerical calculation of mobile work machine part. Manufacturing Technology 18(2), 2018, pp. 190-193.
[21] Lipinski T., Karpisz D. Effect of 80% water solution of animal slurry on carbon structural S235JRC steel at room temperature. Engineering for Rural Development 20, 2021, pp. 1088-1094.
[22] Selejdak, J. 2003, Influencing factors onto quality of welded pipes. Metalurgija, 42 (1), 65-67.
[23] Dvorský D., Kubásek J., Vojtěch D. Microstructure, mechanical and corrosion properties of extruded milled magnesium powder. Manufacturing Technology 20(6), 2020, pp. 708-713.
[24] Abdelmseeh V.A., Jofriet J., Hayward G. Sulphate and sulphide corrosion in livestock buildings, Part I: Concrete deterioration. Biosystems Engineering 99 (2008) 372-381.
[25] Tang X., Xu L.Y., Cheng Y.F. Electrochemical corrosion behavior of X-65 steel in the simulated oil–sand slurry. Synergism of erosion and corrosion. Corrosion Science, 50, 2008, pp. 1469–1474.
[26] Lu B.T., Lu J.F., Luo J.L. Erosion–corrosion of carbon steel in simulated tailing slurries. Corrosion Science, 53, 2011, pp. 1000–1008.
[27] Aguirre J., Walczak M. Effect of dissolved copper ions on erosion–corrosion synergy of X65 steel in simulated copper tailing slurry. Tribology International, 114, 2017, pp. 329–336.
[28] Yang Y., Cheng Y.F. Parametric effects on the erosion–corrosion rate and mechanism of carbon steel pipes in oil sands slurry. Wear 276– 277, 2012, pp. 141– 148.
[29] Song F. G., Du L.G. Erosion corrosion of low-alloy wear-resistant steels in alkaline slurry. Journal of Ironand Steel Research, International 24, 2017, pp. 1065-1072.
[30] Lipiński T. Corrosion Effect of Animal Slurry on Low Carbon S235JR Steel at 333 K. Proceedings of the 8th International Scientific Conference Rural Development 2017, Lithuania 23-24 November, pp. 352-358.
[31] Lipiński T., Karpisz D. Effect of animal slurry on carbon structural S235JR steel at 303 K. 19th International Scientific Conference Engineering for Rural Development, Jelgava, 20-22.05.2020. Proceedings, vol. 19, pp. 1482-1487.
[32] Dudek A., Wlodarczyk R. Structure and properties of bioceramics layers used for implant coatings. Solid State Phenomena 165, 2010, pp. 31-36.
[33] Szczotok A., Pietraszek J., Radek N. Metallographic Study and Repeatability Analysis of γ' Phase Precipitates in Cored, Thin-Walled Castings Made from IN713C Superalloy. Archives of Metallurgy and Materials 62/2, 2017, pp. 595-601.
[34] Antosz K., Pacana A. Comparative analysis of the implementation of the SMED method on selected production stands. Tehnicki Vjesnik 25, 2018, pp. 276-282.
[35] Pacana A., Ulewicz R. Analysis of causes and effects of implementation of the quality management system compliant with iso 9001. Polish Journal of Management Studies 21/1, 2020, pp. 283-296.
[36] Baryshnikova N., Kiriliuk O., Klimecka-Tatar D. Enterprises' strategies transformation in the real sector of the economy in the context of the COVID-19 pandemic. Production Engineering Archives 27/1, 2021, pp. 8-15.

[37] Pietraszek J., Gądek-Moszczak A., Radek N. The estimation of accuracy for the neural network approximation in the case of sintered metal properties. Studies in Computational Intelligence 513, 2014, pp. 125-134.
[38] Pietraszek J., Radek N., Goroshko A.V. Challenges for the DOE methodology related to the introduction of Industry 4.0. Production Engineering Archives 26(4), 2020, 190-194.
[39] PN-EN ISO 683-1:2018-09. Heat treatment steels, alloyed steels and free-cutting steels.
[40] PN-EN ISO 3651-1:2004. Determination of resistance to intergranular corrosion of corrosion-resistant steels. Part 1: Austenitic and ferritic-austenitic (duplex) corrosion-resistant steels.